

# A micromachined inline type microwave power sensor with working state transfer switches\*

Han Lei(韩磊)<sup>†</sup>

Key Laboratory of MEMS of Ministry of Education, Southeast University, Nanjing 210096, China

**Abstract:** A wideband 8–12 GHz inline type microwave power sensor, which has both working and non-working states, is presented. The power sensor measures the microwave power coupled from a CPW line by a MEMS membrane. In order to reduce microwave losses during the non-working state, a new structure of working state transfer switches is proposed to realize the two working states. The fabrication of the power sensor with two working states is compatible with the GaAs MMIC (monolithic microwave integrated circuit) process. The experimental results show that the power sensor has an insertion loss of 0.18 dB during the non-working state and 0.24 dB during the working state at a frequency of 10 GHz. This means that no microwave power has been coupled from the CPW line during the non-working state.

**Key words:** microwave power sensor; micromachined; GaAs MMIC; transfer switches

**DOI:** 10.1088/1674-4926/32/5/055003

**EEACC:** 2575; 8460

## 1. Introduction

Power detection is an important part of microwave and millimeter wave wireless applications. Modern personal communication systems and radar systems require that the power sensor has low volume, reflection losses, insertion losses and power consumption, and can also be fabricated compatibly with the GaAs MMIC or Si processes<sup>[1]</sup>. Existing technology for measuring the microwave and millimeter wave power is based on thermistors, thermocouples and diodes. These are the terminating devices and the signal is not available after power detection. Recently, three sensing principles of inline type microwave power sensors based on MEMS technology were proposed. The first principle utilizes the conversion of microwave power into heat, resulting in a local temperature increase due to ohmic losses from a CPW line's center conductor<sup>[2–4]</sup>. The structure of this sensor is complex and not compatible with the GaAs or Si processes. The second principle was realized by movement detection of a suspended membrane over a CPW line through which the signal is transmitted<sup>[5–9]</sup>. The output of such a power sensor is related to capacitance change, so it needs to be read by the electronics and its performance is strongly dependent of this process. Furthermore, when the microwave power transmitted through the membrane is increased, the reflection and the insertion losses will also increase due to the capacitance change. The two above principles have a trade-off between microwave performance and sensitivity. The third principle couples a small ratio of the microwave power through a MEMS membrane suspended over a CPW line. The coupled microwave power is then converted to heat by the matched resistance and measured by the thermopiles<sup>[10, 11]</sup>. This power sensor has two independent steps: the coupled step and the measurement step. The two steps make it possible for the microwave properties and the sensitivity of the power sensor to

be designed separately. It also means that the power sensor can realize high sensitivity with low insertion losses and reflection losses. The sensor can be used in the middle of the signal chain with a small size and low losses.

In this paper, the theory, design, fabrication and measurements from the microwave power sensor of the third principle with the working state transfer switches are presented. By adding the transfer switches directly at the two sides of the MEMS membrane, a power sensor with two working states is obtained. The novel structure can avoid unnecessary microwave losses during the non-working state. This power sensor has many advantages, such as working state alternation, high sensitivity, wide frequency range, low insertion losses and reflection losses, excellent linearity and it is compatible with the GaAs MMIC process. The experimental results show that the power sensor has an insertion loss of 0.18 dB during the non-working state and 0.24 dB during the working state at 10 GHz frequency. It means that no microwave power has been coupled from the CPW line during the non-working state.

## 2. Principle of operation

### 2.1. Basic operation

An inline type microwave power sensor is composed of a microwave power coupler and a thermoelectric microwave power sensor. Figure 1 shows a schematic view of the power sensor. A membrane is suspended over the CPW line and the capacitance between the membrane and the center conductor of the CPW line couples a small ratio of the microwave power transmitted in the CPW line. The capacitance  $C$  can be expressed as<sup>[12]</sup>

\* Project supported by the National Natural Science Foundation of China (No. 60676043) and the National High Technology Research and Development Program of China (No. 2007AA04Z328).

<sup>†</sup> Corresponding author. Email: hanlei@seu.edu.cn

Received 6 September 2010, revised manuscript received 12 November 2010

© 2011 Chinese Institute of Electronics

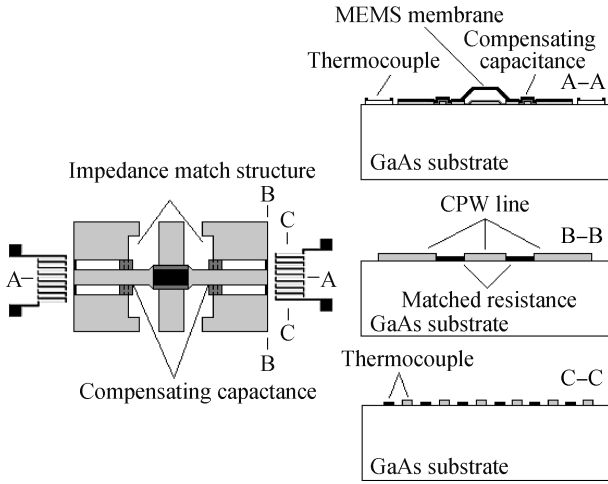


Fig. 1. Schematic view of the inline type microwave power sensor.

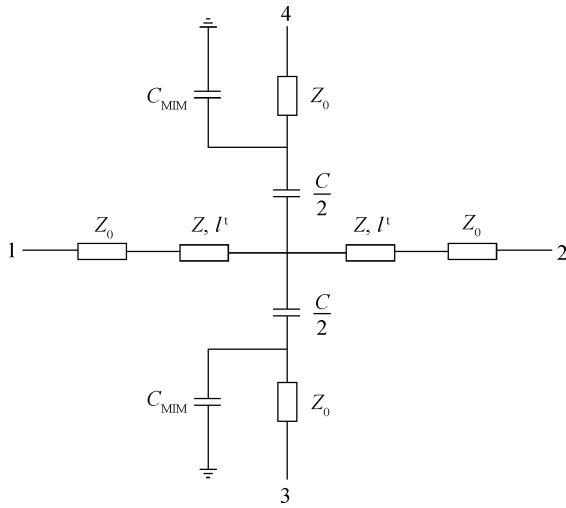


Fig. 2. The lumped element model of the inline type microwave power sensor.

$$C = \frac{\varepsilon_0 b w}{g_0 + \frac{t_d}{\varepsilon_r}} + C_f, \quad (1)$$

where  $b$  is the width of the MEMS membrane,  $w$  is the width of the center conductor of the CPW line,  $g_0$  is the MEMS membrane height,  $t_d$  is the thickness of the insulation layer and  $C_f$  is the fringing field capacitance of the MEMS membrane, which is about 20%–50% of the total capacitance.  $\varepsilon_0$  and  $\varepsilon_r$  are the permittivity of free space and the permittivity of the insulation layer, respectively. Due to the principle of the microwave power sensor, the capacitance  $C$  is needed to couple the microwave power. It is affected by an increase in reflection losses and a variation in coupling during the frequency. In order to obtain low reflection losses and insertion losses, as well as the wideband response, the gap size of the CPW line directly before and after the MEMS membrane is increased and a compensating capacitance is added. Figure 2 shows the lumped element model of the power sensor with the compensating structures.  $C$  is the capacitance between the MEMS membrane and the center conductor of the CPW line,  $C_{MIM}$  is the compensating capacitor,  $Z_0$  is the characteristic impedance of the CPW

line,  $Z$  is the characteristic impedance of the CPW line before and after the capacitance, and  $l'$  is the length of the CPW line before and after the MEMS membrane.

The  $S$  parameters of the power sensor with the compensating structures can be expressed as

$$S_{11} = \left[ -\omega C Z Z_0^2 (\omega C_{MIM} Z_0 - j) \cos^2(\beta l') + \omega C Z^3 (j - \omega C_{MIM} Z_0) \sin^2(\beta l') + \frac{1}{2} (Z^2 - Z_0^2) (\omega C Z_0 + 2\omega C_{MIM} Z_0 - 2j) \times \sin(2\beta l') \right] \times \left\{ [Z_0 \cos(\beta l') + j Z \sin(\beta l')] \times [Z(-2 - 2j\omega C_{MIM} Z_0 + \omega C Z_0 (\omega C_{MIM} Z_0 - 2j))] \cos(\beta l') + [\omega C Z^2 + (2C_{MIM} + C) \omega Z_0^2 + j Z_0 (\omega^2 C C_{MIM} Z^2 - 2)] \sin(\beta l') \right\}^{-1}, \quad (2)$$

$$S_{21} = -[Z Z_0 (j\omega C Z_0 + 2j\omega C_{MIM} Z_0 + 2)] \times \left\{ [Z_0 \cos(\beta l') + j Z \sin(\beta l')] \times [Z(-2 - 2j\omega C_{MIM} Z_0 + \omega C Z_0 (\omega C_{MIM} Z_0 - 2j))] \cos(\beta l') + [\omega C Z^2 + (2C_{MIM} + C) \omega Z_0^2 + j Z_0 (\omega^2 C C_{MIM} Z^2 - 2)] \sin(\beta l') \right\}^{-1}, \quad (3)$$

$$S_{31} = S_{41} = [\omega C Z Z_0 \cos(\beta l') (Z \tan(\beta l') - j Z_0)] \times \left\{ [Z_0 \cos(\beta l') + j Z \sin(\beta l')] \times [Z(-2 - 2j\omega C_{MIM} Z_0 + \omega C Z_0 (\omega C_{MIM} Z_0 - 2j))] \cos(\beta l') + [\omega C Z^2 + (2C_{MIM} + C) \omega Z_0^2 + j Z_0 (\omega^2 C C_{MIM} Z^2 - 2)] \sin(\beta l') \right\}^{-1}, \quad (4)$$

where<sup>[12]</sup>

$$C_{MIM} = \frac{\varepsilon_0 \varepsilon_r b' w'}{t_d}, \quad (5)$$

where  $b$  is the width of the MEMS membrane,  $w$  is the width of the center conductor of the CPW line,  $b'$  is the width of the ground of the CPW line formed as the bottom plate of the compensating capacitor,  $w'$  is the width of the top plate of the compensating capacitor,  $g_0$  is the membrane height,  $t_d$  is the thickness of the insulation layer, and  $\varepsilon_0$  and  $\varepsilon_r$  are the permittivity of free space and the permittivity of the insulation layer, respectively. The matched impedance  $Z$  can be calculated as

$$Z^3 \omega C \tan^2(\beta l') - 2Z^2 \tan(\beta l') + Z Z_0^2 \omega C + 2Z_0^2 \tan(\beta l') = 0. \quad (6)$$

The coupled microwave power is converted to heat by a matched resistance and leads to a temperature increase around the matched resistance. The thermopiles detect the resultant

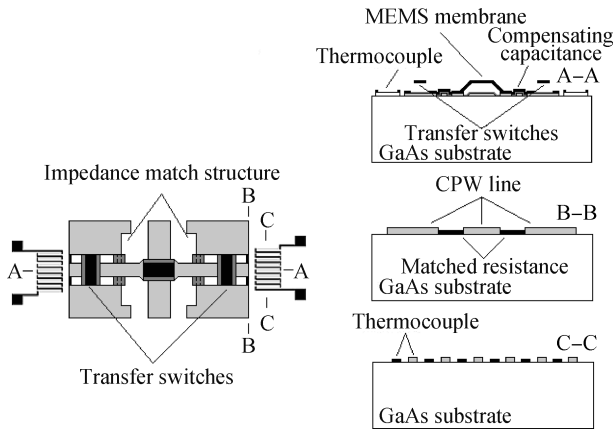


Fig. 3. Schematic view of the inline type microwave power sensor with the working state transfer switches.

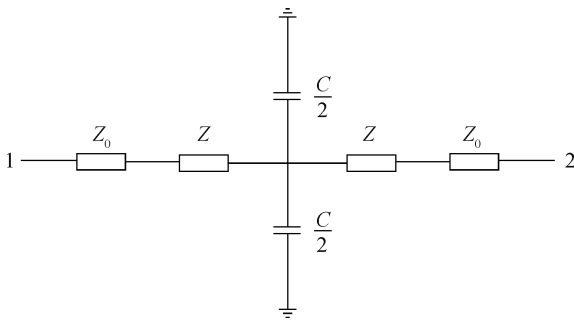


Fig. 4. The lumped element model of the inline type microwave power sensor with the working state transfer switches during the non-working state.

temperature increase of the load and convert the temperature difference to electric signal to realize the microwave power measurement. The thermopiles output thermovoltage and the sensitivity of the thermoelectric microwave power sensor are represented as<sup>[13]</sup>

$$V_{\text{out}} = \alpha \sum_i^{N_i} (T_h - T_c), \quad (7)$$

$$S_{\text{th}} = V_{\text{out}}/P_{\text{diss}}, \quad (8)$$

where  $\alpha$  is the Seebeck coefficient,  $P_{\text{diss}}$  is the microwave power dissipated by the matched resistance, and  $T_h$  and  $T_c$  are the temperature of the hot and cold junction of each thermocouple, respectively. The total sensitivity for the inline type microwave power sensor is obtained by

$$S_{\text{total}} = V_{\text{out}}/P_{\text{total}} = \alpha \sum_i^{N_i} (T_h - T_c)/P_{\text{total}}, \quad (9)$$

where  $P_{\text{total}}$  is the input microwave power transmitted in the CPW line. Since the output thermovoltage is proportional to the input microwave power at the same frequency, a linear relationship between the microwave power and output thermovoltage is expected.

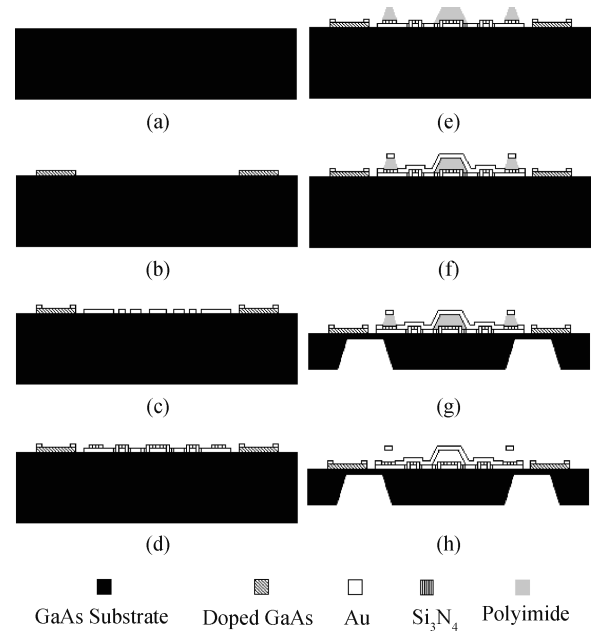


Fig. 5. Fabrication process of the power sensor.

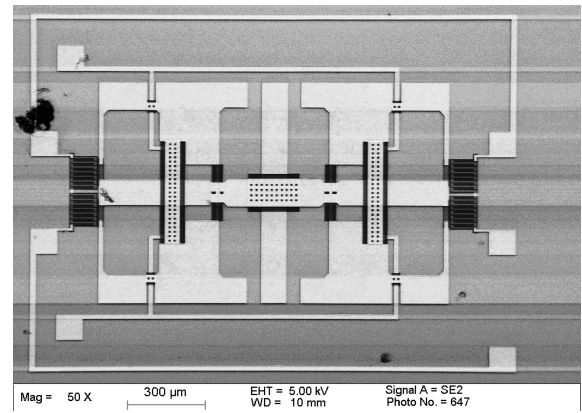


Fig. 6. SEM photo of the fabricated power sensor.

## 2.2. The working state transfer switch structures

In order to obtain both working states of the power sensor, the working state transfer switches, which are located at both sides of the MEMS membrane, are added. The power sensor is at the non-working state when the transfer switches are at the “off” state. Figure 3 shows a schematic view of the power sensor with the working state transfer switches. Figure 4 shows the lumped element model of the power sensor with the working state transfer switches during the non-working state. The lumped element model and  $S$  parameters of the power sensor during the working state are the same as the basic structure.

The  $S$  parameters of the power sensor during the non-working state can be expressed as

$$S_{11} = -\{\omega C Z Z_0^2 \cos^2(\beta l') + \sin(\beta l')[(Z_0^2 - Z^2) \times \cos(\beta l') + \omega C Z^3 \sin(\beta l')]\} \times \{[Z_0 \cos(\beta l') + j Z \sin(\beta l')][Z(\omega C Z_0 - j) \times \cos(\beta l') + (Z_0 + j \omega C Z^2) \sin(\beta l')]\}^{-1}, \quad (10)$$

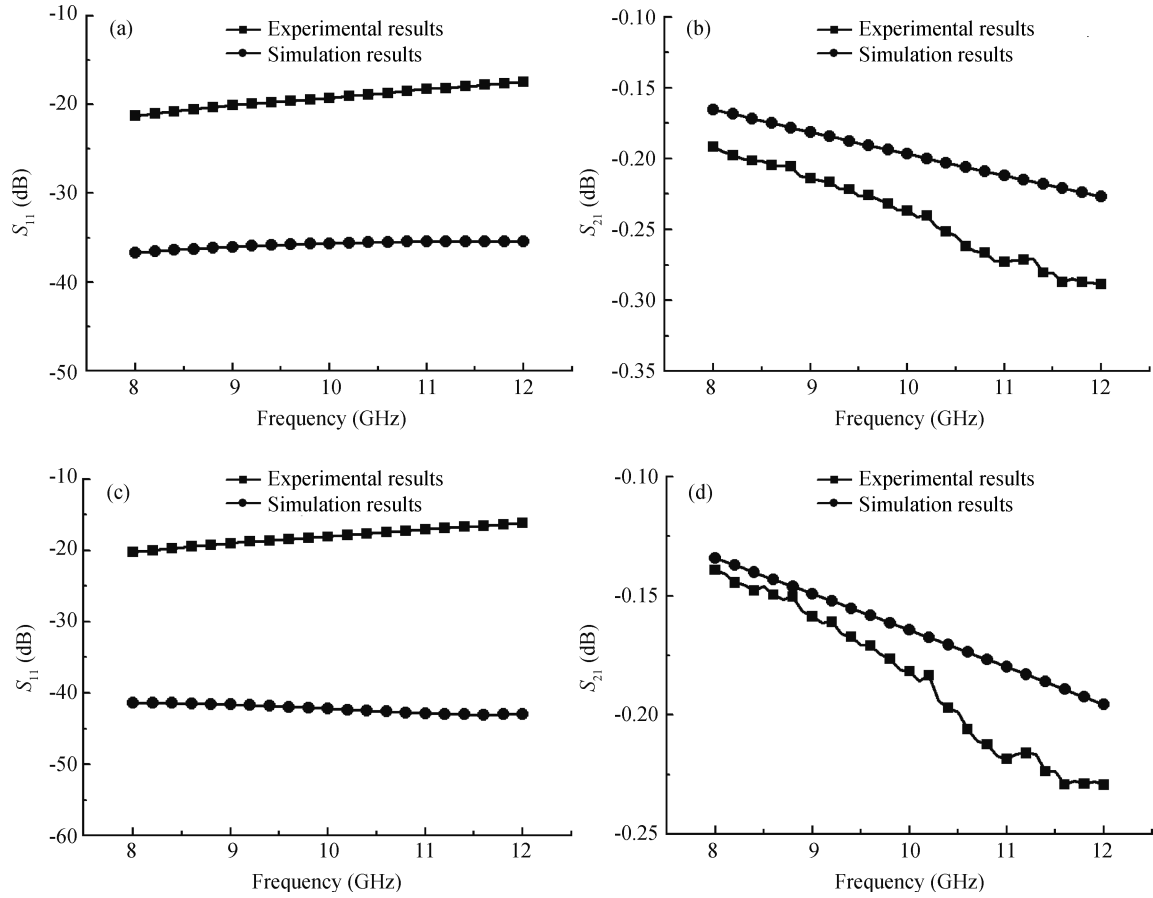


Fig. 7. Experimental results of the power sensor with the transfer switches. (a)  $S_{11}$  at the working state. (b)  $S_{21}$  at the working state. (c)  $S_{11}$  at the non-working state. (d)  $S_{21}$  at the non-working state.

$$S_{21} = -jZ Z_0 \times \{ [Z_0 \cos(\beta l') + jZ \sin(\beta l')] [Z(\omega C Z_0 - j) \times \cos(\beta l') + (Z_0 + j\omega C Z^2) \sin(\beta l')] \}^{-1}. \quad (11)$$

### 3. Design and fabrication

The ratio of the coupled microwave to the total microwave power is designed to be 1%. According to the above formulas, in order to obtain better microwave properties, the dimensions of the compensating structures can be designed as follows.

$$\begin{aligned} Z_0 &= 50 \, \Omega, \quad Z = 75.3 \, \Omega, \quad l' = 330 \, \mu\text{m}, \\ b &= 110 \, \mu\text{m}, \quad w = 100 \, \mu\text{m}, \quad b' = 10 \, \mu\text{m}, \\ w' &= 78 \, \mu\text{m}, \quad g_0 = 1.6 \, \mu\text{m}, \quad t_d = 0.1 \, \mu\text{m}. \end{aligned}$$

The width of the transfer switches is designed to be 80  $\mu\text{m}$ , the height of the transfer switches is designed to be 1.6  $\mu\text{m}$ . The capacitance of the transfer switch at the “OFF” state is about 5 pF, which acts as a small impedance at X-band.

The fabrication of the power sensor is compatible with the GaAs MMIC process<sup>[14]</sup>. The thermopiles were made of gold and  $n^+$  GaAs with a doping concentration of  $1.0 \times 10^{18} \text{ cm}^{-3}$ . The gold was made by sputtering of a 0.3  $\mu\text{m}$  thick gold layer, and the  $n^+$  GaAs was made of an ion implantation layer. The matched resistance was made using a liftoff process

through sputtering of a TaN layer with square resistance of 25  $\Omega/\square$ . The CPW line was designed to have a 50  $\Omega$  characteristic impedance. The CPW line was defined by using a liftoff process through evaporating 500/300/3500/500  $\text{\AA}$  Ti/Pt/Au/Ti layer. The dielectric 1000  $\text{\AA}$  SiN layer was then deposited and patterned. Following that, the 1.6  $\mu\text{m}$  thick polyimide sacrificial layer was deposited and patterned, the thickness of the polyimide layer determines the height of the MEMS membrane and the transfer switches. Finally, a 500/1500/300  $\text{\AA}$  Ti/Au/Ti seed layer was evaporated and patterned. To remove the top Ti layer, the membrane and the transfer switches were electroplated with a 2  $\mu\text{m}$  thick gold layer in a 55° cyanide-based solution. The thickness of the GaAs substrate was decreased to 100  $\mu\text{m}$  using a wafer grinding process, and the substrate underneath the hot thermocouple junctions and the matched resistance was removed via hole etching technology. The sacrificial layer of polyimide was removed using developer, and alcohol was utilized to get rid of the residual water in the MEMS membrane and the transfer switches. Figure 5 shows a summary of the fabrication scheme. A SEM photo of the fabricated power sensor is shown in Fig. 6.

### 4. Experimental results

The  $S$ -parameter measurements are needed for the characterization of the power sensor. The  $S$ -parameter measurements involve measurement of the reflection losses ( $S_{11}$ ) and the in-

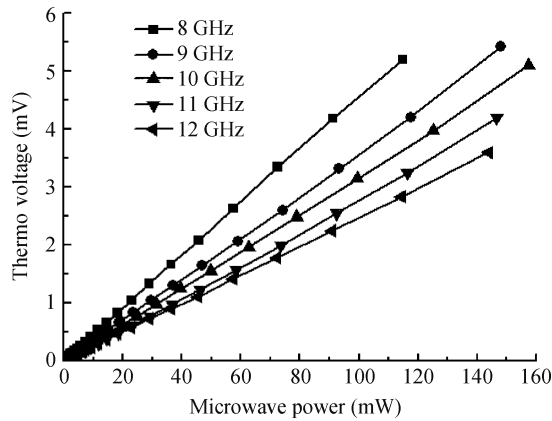


Fig. 8. Experimental results of the output thermovoltages for the power sensor as a function of microwave power at difference frequencies.

sersion losses ( $S_{21}$ ) of the signal applied to the sensor.

The microwave characterization involves measurement of the  $S$ -parameters with a HP8510C vector network analyzer and a Cascade Microtech 1200 probe station. The frequency range is from 8 to 12 GHz. Figures 7 shows the experimental results of the  $S_{11}$  and  $S_{21}$  parameters of the power sensor at the working state and the non-working state.

From Figs. 7(a) and 7(c) we can see that the reflection losses of the power sensor both at the working state and the non-working state are below  $-17$  dB up to 12 GHz and there is nearly no variation of the value. This means that the compensating structures can obtain the low reflection losses both at the working state and the non-working state. From Figs. 7(b) and 7(d) we can see that the insertion losses of the non-working state are less than the insertion losses of the working state by up to 12 GHz. The decrease of the insertion losses is equal to the microwave power coupled from the CPW line by the MEMS membrane. It means that no microwave power has been coupled from the CPW line during the non-working state. Compared with the simulation results of the reflection losses and the insertion losses, the experimental results of the reflection losses and the insertion losses are increased. It has three main reasons. Firstly, the measurement system needs careful calibration and the standard test steps. Otherwise, it will lead to an error in the measurement results. Secondly, the transmission line losses of the experimental result, including the ohmic and dielectric losses, have increased compared to the losses of the simulation results. Thirdly, during the removal of the sacrificial layer of polyimide, the MEMS membrane will bend downwards to the substrate due to compression stress in the membrane. It means that the coupled capacitance between the MEMS membrane and the center conductor of the CPW line is increased. It leads to the mismatch of the structure and more microwave power has been reflected and coupled.

From Fig. 8 we can see that the experimental results of the output thermovoltages for the power sensor as a function of microwave power at difference frequencies. The experimental results demonstrate the excellent linearity of the output thermovoltage with respect to the input microwave power. The sensitivity of the power sensor is  $32.4 \mu\text{V/mW}$  at the 10 GHz frequency.

## 5. Conclusion

A wideband 8–12 GHz inline type microwave power sensor with working and non-working states is presented. The novel part of the power sensor is the working state transfer switch structure. The transfer switches can reduce the microwave losses of the power sensor at the “OFF” state. It means that the power sensor can realize two working state transfer and no microwave power has been coupled from the CPW line during the non-working state. The power sensor has been designed and fabricated compatibly with the GaAs MMIC process. By adding transfer switches at both sides of the MEMS membrane, the power sensor can obtain the low insertion losses during the non-working state as well as good microwave properties during the working state. The experimental results show that the reflection losses both at the working state and the non-working state are lower than  $-17$  dB and the insertion losses of the non-working state are less than that of the working state by up to 12 GHz. The sensitivity is  $32.4 \mu\text{V/mW}$  at the 10 GHz frequency.

## References

- [1] Hartnagel H L, Mutamba K. Power sensors for microwave and millimeter-wave frequencies. *Proc Second Joint Symposium on Opto- and Microelectronic Devices and Circuits*, 2002: 134
- [2] Dehe A, Krozer V, Fricke K, et al. Integrated microwave power sensor. *Electron Lett*, 1995, 31: 2187
- [3] Dehe A, Fricke-Neudert K, Krozer V. Broadband thermoelectric microwave power sensors using GaAs foundry process. *Proc IEEE MTT-S Symposium*, 2002: 1829
- [4] Dehe A, Klingbeil H, Krozer V, et al. GaAs monolithic integrated microwave power sensor in coplanar waveguide technology. *Proc IEEE MTT-S Symposium*, 1996: 161
- [5] Fernandez L J, Sese J, Flokstra J, et al. Capacitive MEMS application for high frequency power sensor. *Proc Micromechanics Europe*, 2002: 252
- [6] Fernandez L J, Visser E, Sese J, et al. Radio frequency power sensor based on MEMS technology. *Proc IEEE Sensors Conf*, 2003: 549
- [7] Vaha-Heikkilä T, Kyynäräinen J, Oja A, et al. Capacitive MEMS power sensor. *Proc 3rd Workshop on MEMS for Millimeterwave Communications*, 2002: 336
- [8] Vaha-Heikkilä T, Kyynäräinen J, Dekker J, et al. Capacitive RF MEMS power sensors. *Proc 3rd ESA Workshop On Millimeter Wave Technology and Application: Circuits, System, and Measurement Techniques*, 2003: 503
- [9] Fernandez L J, Wiegerink R J, Flokstra J, et al. A capacitive RF power sensor based on MEMS technology. *J Micromech Microeng*, 2006, 16: 1099
- [10] Han L, Huang Q A, Liao X P. An inline-type microwave power sensor based on MEMS technology. *J Micromech Microeng*, 2007, 17: 2132
- [11] Han L, Huang Q A, Liao X P, et al. A micromachined inline-type wideband microwave power sensor based on GaAs MMIC technology. *J Microelectromech Syst*, 2009, 18(3): 705
- [12] Muldavin J B, Rebeiz G M. High-isolation CPW MEMS shunt switches—Part I: modeling. *IEEE Trans MTT*, 2000, 48(6): 1045
- [13] Milanovic V, Hopcroft M, Zinke C A, et al. Optimization of CMOS MEMS microwave power sensors. *Proc IEEE International Symposium on Circuits and Systems*, 1999: 144
- [14] Zheng W B, Huang Q A, Liao X P, et al. RF MEMS membrane switches on GaAs substrates for X-band applications. *J Microelectromech Syst*, 2005, 14(3): 464